

Yaning Chen *Editor*

# Water Resources Research in Northwest China

 Springer

# Water Resources Research in Northwest China

Yaning Chen  
Editor

# Water Resources Research in Northwest China

 Springer

*Editor*  
Yaning Chen  
Xinjiang Institute of Ecology  
and Geography  
Chinese Academy of Sciences  
Xinjiang  
People's Republic of China

ISBN 978-94-017-8016-2                      ISBN 978-94-017-8017-9 (eBook)  
DOI 10.1007/978-94-017-8017-9  
Springer Dordrecht Heidelberg New York London

Library of Congress Control Number: 2014930889

© Springer Science+Business Media Dordrecht 2014

This work is subject to copyright. All rights are reserved by the Publisher, whether the whole or part of the material is concerned, specifically the rights of translation, reprinting, reuse of illustrations, recitation, broadcasting, reproduction on microfilms or in any other physical way, and transmission or information storage and retrieval, electronic adaptation, computer software, or by similar or dissimilar methodology now known or hereafter developed. Exempted from this legal reservation are brief excerpts in connection with reviews or scholarly analysis or material supplied specifically for the purpose of being entered and executed on a computer system, for exclusive use by the purchaser of the work. Duplication of this publication or parts thereof is permitted only under the provisions of the Copyright Law of the Publisher's location, in its current version, and permission for use must always be obtained from Springer. Permissions for use may be obtained through RightsLink at the Copyright Clearance Center. Violations are liable to prosecution under the respective Copyright Law.

The use of general descriptive names, registered names, trademarks, service marks, etc. in this publication does not imply, even in the absence of a specific statement, that such names are exempt from the relevant protective laws and regulations and therefore free for general use.

While the advice and information in this book are believed to be true and accurate at the date of publication, neither the authors nor the editors nor the publisher can accept any legal responsibility for any errors or omissions that may be made. The publisher makes no warranty, express or implied, with respect to the material contained herein.

Printed on acid-free paper

Springer is part of Springer Science+Business Media ([www.springer.com](http://www.springer.com))

# Preface

With the increasing concern of global environmental and ecological degradation, there has been an urgent need to investigate the related water cycle changes. Designed for both academic and business sectors, this book examines the major issues in water resources research in Northwest China, approximately one fourth of the nation's entire land area and one of the world's largest arid regions. The arid region of Northwest China is characterized by its extremely vulnerable water resources and associated ecological environment. The large alpine snow and ice cover has contributed to the development of numerous inland streams, forming a unique landscape characterized by mountain-oasis-desert ecosystems. Water, largely originated from the mountain areas, has been a most critical factor to drive the energy and mass circulation in this region, which responds sensitively to the global climate change. This book focuses on some possible impacts of climate change on hydrology and water resources in the arid region of Northwest China. The contributing authors for this book include Yaning Chen, Weihong Li, Zongxue Xu, Zhongqin Li, Jianhua Xu, Xianwei Wang, Yanjun Shen, Zhi Li and Huaijun Wang, all of whom are active researchers in water resources research in arid and cold environments.

This book comprises 11 chapters discussing various aspects in water resources research. Specifically, the book begins with an introductory chapter (Chap. 1) discussing the physical geography and socioeconomic aspects in Northwest China. Chaps. 2-7 discuss the climate system and hydrologic system changes, some implications of these changes in relation to potential evapotranspiration, the hydrological cycle, and the spatiotemporal variations of the snow cover and glaciers through remote sensing, geographic information systems, and statistical analysis. Chaps. 8 and 9 focus on the model description and experimental design to interpret the hydro-climatic process, emphasizing the integration of water, climate, and land ecosystems through field observations and computer-based simulations. Chap. 10 examines some extreme hydrological events and presents a study using the historical trend method to investigate the spatial and temporal variability of changing temperature and precipitation extremes in the hyper-arid region of Northwest China. And the Chap. 11 of this book discusses some possible strategies for sustainable watershed management. We believe that the lessons from this study area can be useful for other arid areas in the world.

The research reported in this book has been supported by the National Basic Research Program of China (973 Program: 2010CB951003). The Editor is grateful to all of those who contributed papers and revised their papers one or more times and those who reviewed papers according to our requests and timelines. The book project would not have been completed without the help and assistance from several staff members at Springer, especially Margaret Deignan and Takeesha Moerland-Torpey. Acknowledges are due to Dr. Xiaojun Yang for his help in many ways.

Urumqi, Xingjiang, China  
15 July 2013

Yaning Chen

# Contents

<b>1 Exordium</b> .....	1
Yaning Chen	
<b>2 Climate System in Northwest China</b> .....	51
Yaning Chen, Baofu Li and Changchun Xu	
<b>3 Hydrologic System in Northwest China</b> .....	109
Yaning Chen, Baofu Li, Zhongsheng Chen and Yuting Fan	
<b>4 Response of Runoff to Climate Change</b> .....	145
Yaning Chen, Zhongsheng Chen, Baofu Li and Qihu Li	
<b>5 Glacier Change and Its Impact on Water Resources</b> .....	193
Zhongqin Li, Meiping Sun and Puyu Wang	
<b>6 Spatiotemporal Variation of Snow Cover from Space in Northern Xinjiang</b> .....	247
Xianwei Wang, Hongjie Xie and Tiangang Liang	
<b>7 Change of Potential Evapotranspiration and Its Implications to Water Cycle</b> .....	267
Zhi Li, Yanjun Shen, Yaning Chen and Weihong Li	
<b>8 The Nonlinear Hydro-climatic Process: A Case Study of the Tarim Headwaters, NW China</b> .....	289
Jianhua Xu, Yaning Chen and Weihong Li	
<b>9 Climate Change Scenarios and the Impact on Runoff</b> .....	311
Zhaofei Liu and Zongxue Xu	

<b>10 Changes in Extreme Hydrological Events</b> .....	359
Huaijun Wang, Yaning Chen and Guili Sun	
<b>11 Water Resource Management</b> .....	405
Yaning Chen, Yanjun Shen and Weihong Li	
<b>Index</b> .....	441



# Contributors

**Yaning Chen** State Key Laboratory of Desert and Oasis Ecology, Xinjiang Institute of Ecology and Geography, Chinese Academy of Sciences, Urumqi, Xinjiang, China

**Zhongsheng Chen** State Key Laboratory of Desert and Oasis Ecology, Xinjiang Institute of Ecology and Geography, Chinese Academy of Sciences, Urumqi, Xinjiang, China

**Yuting Fan** State Key Laboratory of Desert and Oasis Ecology, Xinjiang Institute of Ecology and Geography, Chinese Academy of Sciences, Urumqi, Xinjiang, China

**Baofu Li** State Key Laboratory of Desert and Oasis Ecology, Xinjiang Institute of Ecology and Geography, Chinese Academy of Sciences, Urumqi, Xinjiang, China

**Qihu Li** College of Geomatics, Xi'an University of Science and Technology, Xi'an, China

**Weihong Li** State Key Laboratory of Desert and Oasis Ecology, Xinjiang Institute of Ecology and Geography, Chinese Academy of Sciences, Urumqi, Xinjiang, China

**Zhi Li** State Key Laboratory of Desert and Oasis Ecology, Xinjiang Institute of Ecology and Geography, Chinese Academy of Sciences, Urumqi, China

**Zhongqin Li** State Key Laboratory of Cryospheric Sciences/Tianshan Glaciological Station, Cold and Arid Regions Environmental and Engineering Research Institute, Chinese Academy of Sciences, Lanzhou, China

**Tiangang Liang** College of Pastoral Agriculture Science and Technology, Lanzhou University, Lanzhou, China

**Zhaofei Liu** Institute of Geographic Sciences and Natural Resources Research, Chinese Academy of Sciences, Beijing, China

Key Laboratory of Water and Sediment Sciences, Ministry of Education, College of Water Sciences, Beijing Normal University, Beijing, China

**Yanjun Shen** Key Laboratory of Agricultural Water Resources, Center for Agricultural Resources Research, Chinese Academy of Sciences, Shijiazhuang, China

**Guili Sun** College of Forestry and Horticulture, Xinjiang Agricultural University, Urumqi, China

**Meiping Sun** College of Geography and Environment Sciences, Northwest Normal University, Lanzhou, China

**Huaijun Wang** State Key Laboratory of Desert and Oasis Ecology, Xinjiang Institute of Ecology and Geography, Chinese Academy of Sciences, Urumqi, China

**Puyu Wang** State Key Laboratory of Cryospheric Sciences/Tianshan Glaciological Station, Cold and Arid Regions Environmental and Engineering Research Institute, Chinese Academy of Sciences, Lanzhou, China

**Xianwei Wang** Center of Integrated Geographic Information Analysis, School of Geography and Planning, and Guangdong Key Laboratory for Urbanization and Geo-simulation, Sun Yat-sen University, Guangzhou, China

**Hongjie Xie** Laboratory for Remote Sensing and Geoinformatics, Department of Geological Science, University of Texas at San Antonio, San Antonio, TX, USA

**Changchun Xu** Key Laboratory of Oasis Ecology, School of Resources and Environmental Science, Xinjiang University, Urumqi, China

**Jianhua Xu** The Research Center for East-West Cooperation in China, The Key Lab of GIScience of the Education Ministry PRC, East China Normal University, Shanghai, China

**Zongxue Xu** Key Laboratory of Water and Sediment Sciences, Ministry of Education, College of Water Sciences, Beijing Normal University, Beijing, China

# List of Figures

<b>Fig. 1.1</b>	The geomorphologic setting and zoning of the arid region in Northwestern China .....	2
<b>Fig. 1.2</b>	Annual precipitation contour map for the arid Northwest region .....	9
<b>Fig. 2.1</b>	Trends in temperature during 1960–2010 .....	59
<b>Fig. 2.2</b>	Time series of temperature and its linear trend in ANC from 1960 to 2010.....	60
<b>Fig. 2.3</b>	The temperature trends at the meteorological stations in the three landscapes for the period 1960–2010.....	60
<b>Fig. 2.4</b>	The temperature trends in different landscapes for period <b>a</b> 1960–1989 and <b>b</b> 1990–2010.....	61
<b>Fig. 2.5</b>	Time series of temperature of snowmelt period and its linear trend for <b>a</b> entire northwest China, <b>b</b> southern Tianshan Mountains, <b>c</b> northern Kunlun Mountains, and <b>d</b> northern Qilian Mountains from 1960 to 2010.....	62
<b>Fig. 2.6</b>	The date of maxima daily temperature (9 day moving mean) in every decade over Aksu River and Yarkand River.....	63
<b>Fig. 2.7</b>	The weather and hydrological stations of rivers in the arid region of northwest China .....	64
<b>Fig. 2.8</b>	Temperature anomalies trends in typical river areas in the arid region of Northwest China .....	65
<b>Fig. 2.9</b>	Seasonal temperature trends in the arid region of Northwest China .....	67
<b>Fig. 2.10</b>	Temperature trends by decade in the arid region of northwest China .....	69
<b>Fig. 2.11</b>	Distribution of Mann–Kendall trends of air temperature: <b>a</b> annual, <b>b</b> spring, <b>c</b> summer, <b>d</b> autumn, <b>e</b> winter .....	71
<b>Fig. 2.12</b>	Regional trends of air temperature at basin scale: <b>a</b> annual, <b>b</b> spring, <b>c</b> summer, <b>d</b> autumn, <b>e</b> winter.....	72
<b>Fig. 2.13</b>	<b>a</b> Minimum temperature distribution and <b>b</b> trend variation Z in the arid region of Northwest China.....	72
<b>Fig. 2.14</b>	<b>a</b> Maximum temperature distribution and <b>b</b> trend variation Z in the arid region of Northwest China.....	73

<b>Fig. 2.15</b>	Relationship between the trends in temperature and elevation, latitude and longitude.....	73
<b>Fig. 2.16</b>	Cumulative sum (CUSUM) charts for annual and seasonal air temperature.....	75
<b>Fig. 2.17</b>	Temperature step changes in <b>a</b> mountains, <b>b</b> oasis, <b>c</b> desert landscapes .....	76
<b>Fig. 2.18</b>	The seasonal importance of temperature changes in different periods (1981–2010, 1984–1995) .....	77
<b>Fig. 2.19</b>	The Siberian High Intensity and the winter temperature in the arid region of northwest China.....	78
<b>Fig. 2.20</b>	The winter temperature in the arid region of northwest China and the yearly carbon dioxide emission in China.....	79
<b>Fig. 2.21</b>	Relationships between proportional changes of <b>a</b> annual Siberian High Index (SHI), CDE and winter temperature for the arid region of northwest China, <b>b</b> relationships between proportional changes of CDE and annual temperature for the arid region of northwest China .....	79
<b>Fig. 2.22</b>	Wavelet time-frequency distribution ( <i>left</i> ) and variance ( <i>right</i> ) of temperature in the four headstreams of Tarim river basin <b>a</b> Aksu River, <b>b</b> Yarkant River, <b>c</b> Hotan River, <b>d</b> Kaidu River .....	82
<b>Fig. 2.23</b>	Relations between simulated and measured values of temperature.....	84
<b>Fig. 2.24</b>	Temperature variations in each river area in different periods.....	84
<b>Fig. 2.25</b>	Trends in precipitation during 1960–2010 .....	86
<b>Fig. 2.26</b>	The precipitation trend of each meteorological station during the period 1960 to 2010 .....	86
<b>Fig. 2.27</b>	The precipitation trend of each the meteorological station during the periods <b>a</b> 1960–1986, and <b>b</b> 1987–2010 .....	87
<b>Fig. 2.28</b>	Time series of precipitation of the snowmelt period and its linear trend for <b>a</b> entire northwest China, <b>b</b> southern Tianshan Mountains, <b>c</b> northern Kunlun Mountains, <b>d</b> northern Qilian Mountains.....	88
<b>Fig. 2.29</b>	Precipitation anomalies trends in typical river areas of the arid region of Northwest China.....	89
<b>Fig. 2.30</b>	Precipitation changes of each river in different periods in the arid region of China.....	90
<b>Fig. 2.31</b>	Seasonal precipitation trends (1960–2010) in the arid region of northwest China .....	92
<b>Fig. 2.32</b>	Precipitation trends (1960–2010) in different decades in the arid region of northwest China.....	94
<b>Fig. 2.33</b>	Distribution of Mann–Kendall trends of annual and seasonal precipitation, <b>a</b> annual, <b>b</b> spring, <b>c</b> summer, <b>d</b> autumn, <b>e</b> winter.....	96
<b>Fig. 2.34</b>	Regional trends of precipitation at basin scale <b>a</b> annual, <b>b</b> spring, <b>c</b> summer, <b>d</b> autumn, <b>e</b> winter .....	97

<b>Fig. 2.35</b>	<b>a</b> Relationships between the trends in precipitation and elevation, <b>b</b> latitude, <b>c</b> longitude.....	97
<b>Fig. 2.36</b>	Cumulative sum (CUSUM) charts for annual and seasonal precipitation .....	98
<b>Fig. 2.37</b>	Step change of precipitation in <b>a</b> mountains, <b>b</b> oasis, <b>c</b> desert areas .....	99
<b>Fig. 2.38</b>	Wavelet time-frequency distribution ( <i>left</i> ) and variance ( <i>right</i> ) of precipitation in the four headstreams of the Tarim River Basin <b>a</b> Aksu River; <b>b</b> Yarkant River; <b>c</b> Hotan River; <b>d</b> Kaidu River .....	101
<b>Fig. 2.39</b>	Relations between simulated and measured values of precipitation .....	102
<b>Fig. 2.40</b>	Runoff variations of each river in different periods in the arid region .....	102
<b>Fig. 2.41</b>	Reconstructed <b>a</b> AMT of Jinghe, <b>b</b> ANP at Wusu in northern Xinjiang.....	104
<b>Fig. 3.1</b>	<b>a</b> Distribution of meteorological station and hydrological station; <b>b</b> hydrological basin and drainage basin.....	112
<b>Fig. 3.2</b>	Spatial distribution of annual trends for runoff.....	114
<b>Fig. 3.3</b>	The hydrological stations of rivers in the arid region of northwest China .....	115
<b>Fig. 3.4</b>	Runoff anomalies trends in typical river areas of the arid region of northwest China (Li et al. 2012).....	116
<b>Fig. 3.5</b>	Runoff variations of each river in different periods (before 1990 and after 1990) in the arid region of northwest China (Li et al. 2012).....	117
<b>Fig. 3.6</b>	The changes of runoff ( $\text{m}^3/\text{s}$ ) in Aksu river ( <b>a</b> ), Kaidu river ( <b>b</b> ), Yarkand river ( <b>c</b> ), and Hotan river ( <b>d</b> ) in Xinjiang .....	117
<b>Fig. 3.7</b>	The wavelet approximations for annual runoff in the Hotan River at different time scales. <b>a</b> The diagram of $\ln C(r)$ versus $\ln(r)$ . <b>b</b> The correlation exponent ( $d$ ) versus embedding dimension ( $m$ )...	118
<b>Fig. 3.8</b>	Step change point of runoff in Aksu river ( <b>a</b> ), Kaidu river ( <b>b</b> ), Yarkand river ( <b>c</b> ), and Hotan river ( <b>d</b> ) .....	120
<b>Fig. 3.9</b>	The time-frequency distribution of wavelet coefficient and variance for temperature, precipitation and runoff in Aksu River, respectively (form <i>top to bottom</i> ).....	121
<b>Fig. 3.10</b>	The time-frequency distribution of wavelet coefficient and variance for temperature, precipitation and runoff in Yarkand River, respectively (form <i>top to bottom</i> ).....	122
<b>Fig. 3.11</b>	The time-frequency distribution of wavelet coefficient and variance for temperature, precipitation and runoff in Hotan River, respectively (form <i>top to bottom</i> ) .....	124
<b>Fig. 3.12</b>	The time-frequency distribution of wavelet coefficient and variance for temperature, precipitation and runoff in Kaidu River, respectively (form <i>top to bottom</i> ).....	125

**Fig. 3.13** Variation of annual baseflow and baseflow index for the four headstreams of the Tarim River. **a** Aksu River. **b** Hotan River. **c** Yakand River. **d** Kaidu River ..... 130

**Fig. 3.14** Baseflow separation at the four headstreams of the Tarim River for typical dry and wet years. **a1** Aksu River in a dry year 1986 with SBFI=12.7%. **a2** Aksu River in a wet year 1996 with SBFI=12.5%. **b1** Hotan River in a dry year 1985 with annual SBFI=8.0%. **b2** Hotan River in a wet year 1987 with SBFI=10.8%. **c1** Yakand River in a dry year 1978 with SBFI=13.0%. **c2** Yakand River in a wet year 2007 with SBFI=21.5%. **d1** Kaidu River in a dry year 1980 with SBFI=30.0%. **d2** Kaidu River in a wet year 1981 with SBFI=37.0% ..... 131

**Fig. 3.15** Location map of the Tizinafu River and water sampling locations referred to in this paper ..... 132

**Fig. 3.16** Projections of Akesu river annual runoff and climate factor of wavelet coefficients in Aksu river (**a**), Yarkand River (**b**), Hotan River (**c**), and Kaidu river (**d**) ..... 136

**Fig. 3.17** The typical river runoff variation under different scenarios ..... 138

**Fig. 3.18** The change trends of annual mean temperature and annual precipitation in the Kaidukongque River Basin under different scenarios..... 140

**Fig. 4.1** Correlation between **a** annual runoff and precipitation, and **b** annual runoff and temperature at basin scale..... 147

**Fig. 4.2** The temperature departure of Aksu River (**a**), Yarkand River (**b**), Hotan River (**c**), Kaidu River (**d**), Shule River (**e**), and Shiyang River (**f**)..... 148

**Fig. 4.3** The precipitation departure percentage of Aksu River (**a**), Yarkand River (**b**), Hotan River (**c**), Kaidu River (**d**), Shule River (**e**), and Shiyang River (**f**)..... 149

**Fig. 4.4** The runoff departure of Aksu River (**a**), Yarkand River (**b**), Hotan River (**c**), Kaidu River (**d**), Shule River (**e**), and Shiyang River (**f**)..... 150

**Fig. 4.5** The cycle of (**a1, b1, c1, d1, e1, f1**) precipitation, (**a2, b2, c2, d2, e2, f2**) temperature and (**a3, b3, c3, d3, e3, f3**) runoff. a Aksu River. b Yarkand River. c Hotan River. d Kaidu River. e Shule River. f Heihe River. g Shiyang River..... 153

**Fig. 4.6** Linear fitting of streamflow and precipitation (**a1, b1, c1, d1, e1, f1**), temperature (**a2, b2, c2, d2, e2, f2**) of the Aksu River Basin .... 155

**Fig. 4.7** The change trend of the streamflow of the Yarkand River and Hotan River under different time scales..... 157

**Fig. 4.8** Snow percentage in Tarim River Baisn, south slope of Tianshan and north slope of Kunlun Mountains..... 165

**Fig. 4.9** Relationship between precipitation, snow cover and runoff in Aksu River ..... 166

<b>Fig. 4.10</b>	Time series of precipitation, snow cover (above 4,200 m) and runoff in Aksu River.....	167
<b>Fig. 4.11</b>	The distribution of meteorological and hydrological stations in the ARNC .....	169
<b>Fig. 4.12</b>	Changes of the summer FLH for many years in four typical regions.....	171
<b>Fig. 4.13</b>	Summer runoff changes for many years in four typical regions .....	172
<b>Fig. 4.14</b>	The linear regression between the summer runoff and FLH in four typical regions .....	174
<b>Fig. 4.15</b>	The elastic coefficient and proportion of glacial meltwater runoff in four typical regions .....	176
<b>Fig. 4.16</b>	Runoff before and after step changes in some typical rivers. <b>a</b> Aksu River. <b>b</b> Kaidu River. <b>c</b> Shule River. <b>d</b> Heihe River.....	181
<b>Fig. 4.17</b>	<b>a</b> The relationship between cumulative precipitation and cumulative runoff, <b>b</b> the measured runoff and simulation runoff change during 1994–2010.....	184
<b>Fig. 4.18</b>	Relationships between proportional changes of precipitation and runoff in Kaidu River .....	185
<b>Fig. 4.19</b>	Sensitivity coefficients of annual runoff to the temperature .....	186
<b>Fig. 4.20</b>	Sensitivity coefficients of annual runoff to the precipitation and the change rates of annual runoff caused by the precipitation.....	187
<b>Fig. 5.1</b>	Map of Urumqi River source region, showing locations of Urumqi Glacier No.1, hydrological and meteorological stations .....	196
<b>Fig. 5.2</b>	Annual average air temperature and precipitation and their fitting curves for 1959–2008.....	201
<b>Fig. 5.3</b>	Terminus retreat distance history since 1962 based on directly field measurements .....	203
<b>Fig. 5.4</b>	<b>a</b> Annual cumulative mass balance and <b>b</b> annual equilibrium line altitude of Urumqi Glacier No.1 during 1959–2008.....	204
<b>Fig. 5.5</b>	Interannual changes of glacier runoff, glacier storage, precipitation and evaporation of Urumqi Glacier No.1 from 1959 to 2008.....	205
<b>Fig. 5.6</b>	Interannual change of glacier runoff and discharge at Glacier No.1 gauging station and the glacier runoff contribution to river discharge during 1959–2008 .....	206
<b>Fig. 5.7</b>	Monthly distribution of <b>a</b> average air temperature, precipitation and <b>b</b> discharges of Glacier No.1 and Empty Cirque gauging stations over the period 1959–2008 .....	207
<b>Fig. 5.8</b>	Fitting charts between <b>a</b> discharge of Glacier No.1 gauging station and air temperature <b>b</b> discharge of Empty Cirque gauging station and precipitation.....	207
<b>Fig. 5.9</b>	Time series of modeled and observed discharge for <b>a</b> Glacier No.1 and <b>b</b> Zongkong and gauging stations, of which the daily discharge at the two stations are listed from May to September each year.....	210

<b>Fig. 5.10</b>	Histogram of the residual of <b>a</b> temperature and <b>b</b> precipitation .....	211
<b>Fig. 5.11</b>	Variations of <b>a</b> , <b>b</b> temperature and <b>c</b> , <b>d</b> precipitation derived from downscaling from RegCM3 under SRES A1B scenario for 2041–2060 relative to 2000–2008.....	212
<b>Fig. 5.12</b>	Annual discharge cycle of <b>a</b> Glacier No.1 and <b>b</b> Zongkong catchments simulated by HBV for current climate (2000–2008) and future climate (2041–2060) for three stages of glaciations.....	213
<b>Fig. 5.13</b>	Spatial characteristics of glacier variations in Xinjiang, North Western China .....	221
<b>Fig. 5.14</b>	Sketch map showing the study area and distribution of glaciers .....	229
<b>Fig. 5.15</b>	Example of the glacier outlines extraction from ASTER images and topographic maps. <i>Red</i> glacier outlines are of 2003 and <i>blue</i> outlines of 1956.....	231
<b>Fig. 5.16</b>	Distribution of glacial number and area with different aspects in 2003/2004.....	232
<b>Fig. 5.17</b>	Glacier area, number and area loss by glacier size class for 1956–2003 in the middle Qilian Mountain Region, including the Heihe River Basin and the Beidahe River Basin .....	233
<b>Fig. 5.18</b>	Relative changes in glacier area of different sizes in the middle Qilian Mountain Region from 1956 to 2003. Mean values of glacier area change ( <i>horizontal line</i> ) together with standard deviation (vertical bars) are given for four area classes (in km <sup>2</sup> : 0.01–0.1, 0.1–0.5, 0.5–1.0, 1.0–5.0, > 0.0 .....	234
<b>Fig. 6.1</b>	Predicted spectral reflectance of dry snow surface under clear sky at the Summit station (72.5794 N, 38.5042 W) of Greenland. Snow density is 250.0 kg m <sup>-3</sup> , and snow grain radiuses are 50, 100, 200 and 500 μm from top to bottom, respectively. Finer snow grain size has higher reflectance particularly in the near and mid infrared wavelength range. Detailed model and theory description are documented by Flanner and Zender (2006). The three <i>dashed lines</i> from <i>left</i> to <i>right</i> are the wavelength positions of MODIS band 4, band 6 and band 7, respectively, and the width of the line is proportional to the width of wavelength range ...	249
<b>Fig. 6.2</b>	Terra/Aqua MODIS standard snow cover products. Aqua MODIS snow cover product's names begin with MYD .....	252
<b>Fig. 6.3</b>	Test areas showing elevation distribution on central Tianshan Mountains, indicating by the <i>white</i> polygon. The shaded area on the inset map is the northern Xinjiang, China, with <i>black</i> dots for climate stations of snow depth measurements. The Ili River basin is at the north foot of Central Tianshan Mountains. The Taklamakan Desert is in the south .....	256
<b>Fig. 6.4</b>	Comparison of MODIS mean snow covered duration/days (SCD) and in situ observations of mean SCD at 20 climate stations with ascending order of elevation ( <i>right</i> scale, m) in Northern Xinjiang, China, from 2001 to 2005. The mean	



	agreement is the average Agreements defined in Eq. (6.3) for all 20 stations in the four hydrologic year from 2001–2002 to 2004–2005 .....	258
<b>Fig. 6.5</b>	Spatial distribution of mean snow covered duration/days (SCD) on the Central Tianshan Mountains within the six hydrologic years from 2000 to 2006 .....	259
<b>Fig. 6.6</b>	Spatial distribution of SCD anomaly map in each hydrological year on the Central Tianshan Mountains. The mean SCD map of the 6 years was used as a basis. The <i>white</i> area represents the minimum snow cover or perennial snow in August of each year .....	260
<b>Fig. 6.7</b>	Variation of snow cover index (SCI) on the Central Tianshan Mountains within the six hydrologic years from 2000 to 2006 .....	261
<b>Fig. 6.8</b>	Spatial distribution of snow cover onset dates (SCOD) and end dates (SCED) maps on the Central Tianshan Mountains in the fall and spring seasons of 2004 and 2005, respectively. The <i>white</i> area represents the minimum snow cover or perennial snow in August of each year.....	262
<b>Fig. 7.1</b>	Location of the arid region of northwest China .....	269
<b>Fig. 7.2</b>	Change of pan evaporation ( $E_{pan}$ ) from 1958 to 2001 .....	271
<b>Fig. 7.3</b>	Trends in annual $E_{pan}$ for the meteorological stations in the Northwest China from 1958 to 2001.....	271
<b>Fig. 7.4</b>	Temporal changes of meteorological factors .....	272
<b>Fig. 7.5</b>	Comparison of annual pan evaporation and potential evapotranspiration from 1958 to 2001 .....	274
<b>Fig. 7.6</b>	Change in $ET_0$ in the arid region of Northwest China from 1958 to 2010.....	275
<b>Fig. 7.7</b>	Trends in $ET_0$ in four seasons (DJF, MAM, JJA, SON) from 1958 to 2010.....	276
<b>Fig. 7.8</b>	Trends significance in annual $ET_0$ for the meteorological stations in the Northwest China during the periods (a) 1958–1993, and (b) 1994–2010.....	276
<b>Fig. 7.9</b>	Trends in annual $ET_0$ for the meteorological stations in the Northwest China during the periods (a) 1958–1993, and (b) 1994–2010.....	277
<b>Fig. 7.10</b>	Spatial distribution of climate factors ( $T_a$ , DTR, P and RH) trends identified by Mann–Kendall test in northwest China in 1958–2010. a Trend of $T_a$ in 1958–2010, b Trend of DTR in 1958–2010, c Trend of P in 1958–2010, d Trend of RH in 1958–2010.....	279
<b>Fig. 7.11</b>	Spatial distribution of climate factors (SD and WS) trends identified by Mann–Kendall test in northwest China for the two periods: 1958–1993, 1994–2010. a Trend of SD in 1958–1993, b Trend of SD in 1994–2010, c Trend of WS in 1958–1993, d Trend of WS in 1994–2010.....	280

**Fig. 7.12** Concept of the complementary relationship..... 282

**Fig. 8.1** Location of study area ..... 292

**Fig. 8.2** A plot of  $\ln C(r)$  versus  $\ln (r)$  ..... 299

**Fig. 8.3** The correlation exponent ( $d$ ) versus embedding dimension ( $m$ )..... 299

**Fig. 8.4** The nonlinear variation patterns for AR in the Yarkand River at the different time scales ..... 301

**Fig. 8.5** The nonlinear variation patterns for AAT in the Yarkand River Basin at the different time scales ..... 302

**Fig. 8.6** The nonlinear variation patterns for AP in the Yarkand River Basin at the different time scales ..... 302

**Fig. 8.7** The nonlinear variation patterns of AAT, AP and AR in the Kaidu River at different time scales..... 304

**Fig. 8.8** Simulated results for AR by BPANN and MLR at the different time scales ..... 307

**Fig. 9.1** Location of the Tarim River Basin in China, meteorological stations and the selected NCEP Reanalysis grids used in this study... 316

**Fig. 9.2** Example of ranking 25 GCMs based on BS statistics (GCM IDs could be found in Table 9.1) ..... 319

**Fig. 9.3** Spatial distributions of annual temperature of the TRB, both **a** observed; and **b** simulated by ECHO\_G..... 321

**Fig. 9.4** Empirical cumulative probabilities of observed and modeled monthly mean temperature for the TRB ..... 322

**Fig. 9.5** Boxplots of ensemble PDF-based skill scores of monthly mean air temperature over all grids in the study area ..... 323

**Fig. 9.6** NCEP and GCM monthly precipitation distribution over TRB ..... 326

**Fig. 9.7** Cumulative empirical probabilities of observed and modeled monthly precipitation ..... 327

**Fig. 9.8** Boxplots of ensemble PDF-based skill scores of monthly mean precipitation over all grids of study region ..... 328

**Fig. 9.9** MSLP gradients over the Tarim River basin (*gray* grids mean covering observed stations)..... 331

**Fig. 9.10** BIC with different numbers of hidden states (**a** is for the wet season model; **b** is for the dry season model) ..... 335

**Fig. 9.11** Relative errors between modeled and observed annual precipitation for each station in the model calibration and validation (*'cali'* and *'vali'* mean in the calibration and validation; *gray box* indicate median values at the level of 0.95)..... 336

**Fig. 9.12** Modeled and observed monthly precipitation for both model *calibration* and *validation*..... 337

**Fig. 9.13** Distributions of modeled and observed wet spell length, dry spell length and wet-day precipitation amount in the model calibration and validation (The distributions were fit based on the Gamma distribution; **a, c, e** describe wsl, dsl and wpa in calibration respectively; while **b, d, f** was same as that but for validation)..... 339

<b>Fig. 9.14</b>	Box plots of both <i>inter-annual correlation coefficients</i> for each observed station and <i>spatial correlation coefficients</i> for each month in the model calibration and validation (' <i>cali</i> ' and ' <i>vali</i> ' mean in the calibration and validation; <i>gray box</i> indicate median values at the level of 0.95) .....	340
<b>Fig. 9.15</b>	Interval plots of two skill scores for wet spell length, dry spell length and wet-day precipitation amount of each station in the model calibration and validation ( <b>a</b> and <b>b</b> were for Sscore in the calibration and validation respectively; while <b>c</b> and <b>d</b> were the same as that but for BS) .....	341
<b>Fig. 9.16</b>	Model bias for precipitation and temperature ( <b>a</b> , <b>b</b> describe bias of mean and percentile values for temperature, respectively; <b>c</b> , <b>d</b> are the same as that but for precipitation. " <i>-ca</i> " and " <i>-va</i> " mean calibration and validation respectively; " <i>-c</i> ", " <i>-e</i> ", " <i>-g</i> " mean predictors of CSIRO30, ECHAM5 and GFDL21 respectively; " <i>tx</i> ", " <i>tn</i> " mean maximum and minimum air temperatures respectively; " <i>tn5</i> ", " <i>tx95</i> ", " <i>p95</i> " mean 5th value of minimum air temperature, 95th value of maximum air temperature and wpa, respectively) .....	345
<b>Fig. 9.17</b>	Boxplots for precipitation, maximum and minimum air temperatures based on skill scores ( <b>a</b> , <b>b</b> describe air temperature; <b>c</b> , <b>d</b> describe precipitation. " <i>-ca</i> " and " <i>-va</i> " mean calibration and validation respectively; " <i>-c</i> ", " <i>-e</i> ", " <i>-g</i> " mean predictors of CSIRO30, ECHAM5 and GFDL21 respectively; " <i>tx</i> ", " <i>tn</i> " mean maximum and minimum air temperatures respectively; " <i>tn5</i> ", " <i>tx95</i> ", " <i>p95</i> " mean 5th value of minimum air temperature, 95th value of maximum air temperature and wpa, respectively) .....	345
<b>Fig. 9.18</b>	Changes of mean values for precipitation, maximum and minimum air temperature projected by statistical downscaling models ( <b>a</b> , <b>b</b> , <b>c</b> describe changes of maximum and minimum air temperatures, precipitation, respectively; "46" and "81" represent periods of 2046–2065 and 2081–2100, respectively; " <i>-c</i> ", " <i>-e</i> ", " <i>-g</i> " mean predictors of CSIRO30, ECHAM5 and GFDL21, respectively; " <i>a1b</i> ", " <i>a2</i> " and " <i>b1</i> " represent SRES A1B, A2, and B1, respectively. The following is the same) .....	346
<b>Fig. 9.19</b>	The headwater catchment of the TRB .....	348
<b>Fig. 9.20</b>	Mean monthly hydrographs for calibration and validation periods in headwater catchment of the TRB. (" <b>a</b> " and " <b>b</b> " describe hydrographs for calibration and validation periods, respectively) ....	351
<b>Fig. 9.21</b>	Monthly, seasonal and annual runoff changes under climate change scenarios in the future ( <b>a</b> and <b>b</b> describe periods of 2046–2065 and 2081–2100, respectively) .....	352
<b>Fig. 9.22</b>	Spatial distribution for runoff changes in the HC during the period of 2046–2065 .....	353

<b>Fig. 9.23</b>	Spatial distribution for evapotranspiration changes in the HC during the period of 2046–2065.....	355
<b>Fig. 10.1</b>	Location of the arid region and meteorological stations.....	362
<b>Fig. 10.2</b>	Spatial patterns of trends per decade during 1960–2010 in the arid region of China of cold extremes (FD0, ID0, TN10p, TX10p, TNn and TXn); <i>Upward-pointing (downward pointing) triangles</i> indicate increasing (decreasing) trends.....	365
<b>Fig. 10.3</b>	Regional annual and seasonal trends for temperature indices; The dot line is the 95 % confidence level for Mann–Kendall test ( <i>a, b</i> annual change, <i>c, d</i> seasonal change).....	366
<b>Fig. 10.4</b>	Spatial patterns of trends per decade during 1960–2010 in the arid region of China of the seasonal occurrence of cold nights (TN10p).....	368
<b>Fig. 10.5</b>	The probability distribution of FD0, ID0, TX10p and TN10p, respectively .....	369
<b>Fig. 10.6</b>	Power spectrum of ID0 and TX10 (surrounded by the <i>black line</i> in Figure is significant at 0.05 level. The <i>red</i> -alignment is the high energy spectrum).....	369
<b>Fig. 10.7</b>	Spatial patterns of trends per decade during 1960–2010 in the arid region of China of the warm extremes.....	370
<b>Fig. 10.8</b>	Spatial patterns of trends per decade during 1960–2010 in the arid region of China of but for the seasonal TN90p.....	371
<b>Fig. 10.9</b>	Probability function of warm extremes (TX10p and TN90p, respectively).....	371
<b>Fig. 10.10</b>	Spatial patterns of trends per decade during 1960–2010 in the arid region of China of but for the annual and seasonal diurnal temperature range (DTR).....	372
<b>Fig. 10.11</b>	Spatial distribution of trends ( <i>left</i> column, a1–a4) and trend magnitudes ( <i>right</i> column, b1–b4) of precipitation extremes.....	374
<b>Fig. 10.12</b>	Seasonal spatial trends ( <i>left</i> column, a1–a2) and trend magnitudes for RX1day ( <i>right</i> column, b1–a2).....	374
<b>Fig. 10.13</b>	Regional trends of precipitation extremes.....	375
<b>Fig. 10.14</b>	Location and topography of the research area .....	380
<b>Fig. 10.15</b>	Inter-annual spatial distribution of extreme hydrological events in Xinjiang (abscissa for the month/month; ordinate for the frequency of disaster/times).....	382
<b>Fig. 10.16</b>	The frequency change in various types of extreme hydrological events .....	384
<b>Fig. 10.17</b>	Decadal changes of extreme hydrological events in Xinjiang.....	385
<b>Fig. 10.18</b>	Concentration degree decadal change from 1901 to 2010 in Xinjiang.....	386
<b>Fig. 10.19</b>	The spatial distribution of extreme hydrological events.....	387
<b>Fig. 10.20</b>	The spatial distribution of extreme hydrological events in Xinjiang.....	388

<b>Fig. 10.21</b>	Distribution of the river system in the Tarim River Basin .....	391
<b>Fig. 10.22</b>	Change relation of temperature, precipitation and extreme hydrological events in Xinjiang .....	394
<b>Fig. 10.23</b>	Relationship between hydrological extremes and regional climate .....	395
<b>Fig. 10.24</b>	Wavelet coherence of the hydrological extremes and regional climate .....	396
<b>Fig. 10.25</b>	Distribution probability of Tarim River ( <i>a</i> Aksu River, <i>b</i> Yarkand River, <i>c</i> Hotan River, <i>d</i> Kaidu River) .....	397
<b>Fig. 11.1</b>	The variations of crops irrigated area in northwestern arid region.....	422
<b>Fig. 11.2</b>	Spatial distribution of crop acreage in the Northwestern Arid Region of China and its change (1989–2010).....	423
<b>Fig. 11.3</b>	IWR compared with actual diverted in Kuqa County .....	428
<b>Fig. 11.4</b>	<b>a</b> The spatial distribution of irrigation water demand in the arid region of northwestern China in 2010, and <b>b</b> Its change compared to 1989 .....	429
<b>Fig. 11.5</b>	The intra-annual variation of irrigation water demand in different sub-regions <b>a</b> South Xinjiang, <b>b</b> North Xinjiang, <b>c</b> Heixi Corridor in the northwestern arid region (1989–2010) .....	430
<b>Fig. 11.6</b>	Inter annual variation of irrigation water requirement for different crops and different sub-regions in the northwestern arid region of China.....	431
<b>Fig. 11.7</b>	Changes of crop growing area in the three typical basins .....	432
<b>Fig. 11.8</b>	Typical watershed years average monthly runoff, irrigation water demand and the change of the irrigation water supply and demand in May.....	434
<b>Fig. 11.9</b>	The spatial distribution of water level.....	435

# List of Tables

<b>Table 1.1</b>	Northwest arid area's population composition in 2011 .....	28
<b>Table 1.2</b>	The main ethnic groups in Xinjiang population growth from 1991 to 2011 (Unit: $10^4$ ).....	30
<b>Table 1.3</b>	The Hexi Corridor land desertification: degree and distribution characteristics ( $10^4$ hm <sup>2</sup> ).....	32
<b>Table 2.1</b>	The rivers and weather stations information in the arid region of Northwest China .....	64
<b>Table 2.2</b>	Temperature trends and tests in different typical river areas in the arid region of northwest China.....	66
<b>Table 2.3</b>	The annual and seasonal trend in temperature over different regions .....	68
<b>Table 2.4</b>	Results of Mann–Kendall test for annual and seasonal precipitation and temperature.....	70
<b>Table 2.5</b>	The relationship between seasonal temperature trends and longitude, latitude and elevation .....	74
<b>Table 2.6</b>	The correlation coefficients between the winter temperature in the entire region (the Arid Region of Northwest China), mountains, oases and certain factors that may affect the temperature.....	77
<b>Table 2.7</b>	The statistical characteristics of Siberian High Index, CDE, annual temperature and winter temperature for different period....	80
<b>Table 2.8</b>	Precipitation trends and tests in typical river areas of the arid region of Northwest China .....	90
<b>Table 2.9</b>	The annual and seasonal trend in precipitation over different regions .....	93
<b>Table 2.10</b>	The relationship between seasonal precipitation trends and elevation, longitude, latitude and atmospheric circulation.....	93
<b>Table 2.11</b>	Results of Mann–Kendall test for annual and seasonal precipitation and temperature.....	95
<b>Table 2.12</b>	Precipitation trends and tests in typical river areas of the arid region of northwest China .....	100
<b>Table 2.13</b>	Extreme temperature (T) and precipitation (P) .....	105

<b>Table 3.1</b>	The correlation dimensions for the annual runoff processes in the Hotan, Yarkand and Aksu rivers .....	119
<b>Table 3.2</b>	Hurst exponents for the annual runoff processes in the three headwaters of the Tarim River (Xu et al. 2009) .....	119
<b>Table 3.3</b>	Catchment and baseflow characteristics of the four headwater streams .....	129
<b>Table 3.4</b>	Annual variations of baseflow and BFI for the four headwater streams .....	130
<b>Table 3.5</b>	Spatial characteristics of ice-snowmelt in the Tizinafu River streamflow .....	133
<b>Table 3.6</b>	Temporal characteristics of ice-snowmelt in the Tizinafu River streamflow .....	133
<b>Table 3.7</b>	Fitting equation of temperature, precipitation and runoffwavelet coefficients in Aksu river .....	137
<b>Table 3.8</b>	Fitting equation of temperature, precipitation and runoffwavelet coefficients in Yark- and river .....	137
<b>Table 3.9</b>	Fitting equation of temperature, precipitation and runoffwavelet coefficients in Hotan river .....	137
<b>Table 3.10</b>	Fitting equation of temperature, precipitation and runoffwavelet coefficients in Kaidu river .....	138
<b>Table 3.11</b>	STAR validation: observations and projections, both for the validation period from 1986 to 2010 .....	139
<b>Table 3.12</b>	Annual mean temperature and annual precipitation of Bayinbuluke and Baluntai in 2015, 2025 and 2035 under different scenarios.....	140
<b>Table 3.13</b>	Prediction results of annual runoff in 2015, 2025 and 2035 under different scenarios .....	141
<b>Table 4.1</b>	The regression equations of streamflow and precipitation, temperature under multi-time scales .....	158
<b>Table 4.2</b>	The regression equations of streamflow and precipitation, temperature under multi-time scales of the Hotan River.....	159
<b>Table 4.3</b>	Partial correlation analysis between flow variables (runoff, baseflow, and BFI) and climate factors (temperature and precipitation) for the four rivers .....	163
<b>Table 4.4</b>	Terrain classification coding in MODIS.....	164
<b>Table 4.5</b>	Terrain re-classification coding in MODIS .....	164
<b>Table 4.6</b>	The test results of change trends and abrupt changes of the summer FLH in four typical regions .....	171
<b>Table 4.7</b>	The test results of change trends and abrupt changes of the summer runoff in four typical regions.....	172
<b>Table 4.8</b>	The statistics of rivers runoffcomponentsin four typical regions...	175
<b>Table 4.9</b>	The distribution of glaciers covering four typical regions in ARNC.....	177
<b>Table 4.10</b>	Step changes of runoff time series .....	181

<b>Table 4.11</b>	Runoff changes caused by climate change and human activities...	182
<b>Table 4.12</b>	Sensitivity analysis of runoff to different climate scenarios in the headwater of Tarim River.....	189
<b>Table 5.1</b>	Main geographical and hydrometeorological features of the two catchments.....	197
<b>Table 5.2</b>	Statistically significant coefficients for monthly temperature, precipitation and discharge and year of abrupt change for 1959–2008.....	201
<b>Table 5.3</b>	Glacier area change since 1962.....	202
<b>Table 5.4</b>	Regression analysis of the dependence of discharge on air temperature and precipitation in the ablation period at the two tested sites.....	208
<b>Table 5.5</b>	Changes in precipitation, temperature, glacier mass balance, glacier runoff and river discharge for the periods 1959–1993 and 1994–2008.....	208
<b>Table 5.6</b>	Sensitive parameters and the optimal values of HBV for the two investigated areas.....	209
<b>Table 5.7</b>	Efficiency criterions of modeling performance for the two investigated areas [ $R^2$ is from Eq. (5.2), $RE$ is from Eq. (5.3).....	210
<b>Table 5.8</b>	Parameters of the statistical relationship between the observed and projected data.....	211
<b>Table 5.9</b>	Mean change in future discharge (2041–2060) under A1B emission scenarios relative to the present discharge (2000–2008) for three glaciations stages and for two catchments.....	214
<b>Table 5.10</b>	The investigated glaciers.....	219
<b>Table 5.11</b>	Information of remote sensing images.....	220
<b>Table 5.12</b>	Glacier area changes between 1956 and 2003 in the middle Qilian Mountain Region.....	233
<b>Table 5.13</b>	Comparison of glacier changes in the eastern, middle and western Qilian Mountain Region.....	235
<b>Table 7.1</b>	Climate trends of meteorological factors (/10a).....	278
<b>Table 7.2</b>	Annual complete correlation coefficients between $ET_0$ and climate factors.....	281
<b>Table 8.1</b>	The correlation dimensions for AR in the Tarim headwaters.....	300
<b>Table 8.2</b>	Hurst exponents for AR in the Tarim headwaters.....	300
<b>Table 8.3</b>	Basic parameters of the BPANN for hydro-climatic process in the Kaidu River at different time scales.....	305
<b>Table 8.4</b>	MLREs for hydro-climatic process in the Kaidu River at different time scales.....	305
<b>Table 8.5</b>	Comparison between BPANN and MLR model in the Kaidu River at different time scales.....	308
<b>Table 9.1</b>	Climate models data description.....	317



**Table 9.2** Model performance for monthly mean air temperature ..... 320

**Table 9.3** Model performance for precipitation ..... 325

**Table 9.4** Comparison of Scores for monthly MSLP, mean temperature and precipitation..... 329

**Table 9.5** NCEP/NCAR candidate predictors ..... 330

**Table 9.6** Statistics of mean and percentile values for dry spell length, wet spell length and wet-day precipitation amount in the calibration and validation periods ..... 338

**Table 9.7** Explained variances of each predictor and SDSM and NHMM selected predictors ..... 343

**Table 9.8** Model performance on monthly runoff in calibration and validation periods ..... 350

**Table 10.1** Definitions of 15 temperature indices and 9 indices used in this study, all the indices are calculated by RCLIMDEX ..... 363

**Table 10.2** Percentage of stations showing significant annual trends for each index..... 367

**Table 10.3** Proportion of individual stations where the trend in one index is of greater magnitude than the trend in a second ..... 368

**Table 10.4** Relationship between climate extremes (unit/decade), elevation (m) and mean climate (unit/decade) (the coefficient is the linear slope between two variables; slope significant are marked in bold) ..... 376

**Table 10.5** Trends of temperature and precipitation extremes from this study and other works (Trends significant are marked in bold)... 378

**Table 10.6** The concentration degree of extreme hydrological events in Xinjiang..... 379

**Table 10.7** The concentration index of extreme hydrological events in Xinjiang..... 383

**Table 10.8** Monotonic trend test for temperature, precipitation and extreme hydrological events in Xinjiang ..... 394

**Table 10.9** Two-tailed Wilcoxon testing the correlation among temperature, precipitation and runoff in Yarkant River..... 398

**Table 10.10** The change of the 0 °C level high of the flood peak discharge above 4,000 m<sup>3</sup>/s ..... 398

**Table 10.11** Winter precipitation and cumulative depth of snowpack anomaly before snowmelt occurred (Unit: %) ..... 399

**Table 10.12** Winter temperature anomaly and spring temperature extreme change before snowmelt occurred (°C, °C/d, respectively) ..... 400

**Table 11.1** Water resources in arid areas of Northwest China..... 407

**Table 11.2** Glacier meltwater and their recharge proportions to rivers in the northwest arid area ..... 412

**Table 11.3** Water resources in arid areas of Northwest China..... 417

**Table 11.4** The crop coefficient of the major crops at each growth stage in some sites in northwestern arid area..... 426

<b>Table 11.5</b>	The irrigation efficiency in the study region during past 20 years.....	426
<b>Table 11.6</b>	Annual average crop water demand and its trend test (1989–2010, Unit: mm/y).....	427
<b>Table 11.7</b>	Typical basin runoff characteristics and irrigation water demand (0.1 billion · m <sup>3</sup> /y).....	433

# Chapter 1

## Exordium

Yaning Chen

**Abstract** The arid region of Northwest China is characterized by its extremely vulnerable water resources and associated ecological environment. Water is a critical factor to drive the energy and mass circulation in this region, which responds sensitively to the global climate change. The contradictions between ecology and industrial, agricultural production are very conspicuous in arid region. This chapter discusses the physical geography, climatic characteristics and socioeconomic aspects in Northwest China, the main aspects are as follows: (1) By a waving geomorphic land surface with inter-spacing mountains and depressed basins, the typical landscape comprised vertically with mountain—oasis—desert ecosystems. (2) Situated far from the sea, the relatively secluded Northwest region has a typical continental climate marked by scarce precipitation, high evaporation, wide temperature fluctuations and strong winds. (3) The multicultural population is mainly distributed in the oases, where oasis agriculture is the mainstay. The ecosystems are extremely fragile due mainly to the internal factors of ecological processes and the interference of human activities.

**Keywords** Northwest China · Landform features · Socio-economic characteristics · Population composition · Ecological degradation

### 1.1 Natural Geography

The arid region of Northwest China is located in the hinterland of the Eurasian continent, spanning an area from 35° to 50° N and 73° to 106° E. It lies west of the Helan and Wushao Mountains, north of the Kunlun Mountains, and includes the Tarim River Basin, the Qaidam Basin, the Badan Jaran Desert and the Tengger Desert. Geopolitically, the area incorporates the Xinjiang Uyghur Autonomous

---

Y. Chen (✉)  
State Key Laboratory of Desert and Oasis Ecology,  
Xinjiang Institute of Ecology and Geography,  
Chinese Academy of Sciences, No. 818 South Beijing Road,  
Urumqi 830011 Xinjiang, China  
e-mail: chenyn@ms.xjb.ac.cn

Y. Chen (ed.), *Water Resources Research in Northwest China*,  
DOI 10.1007/978-94-017-8017-9\_1, © Springer Science+Business Media Dordrecht 2014

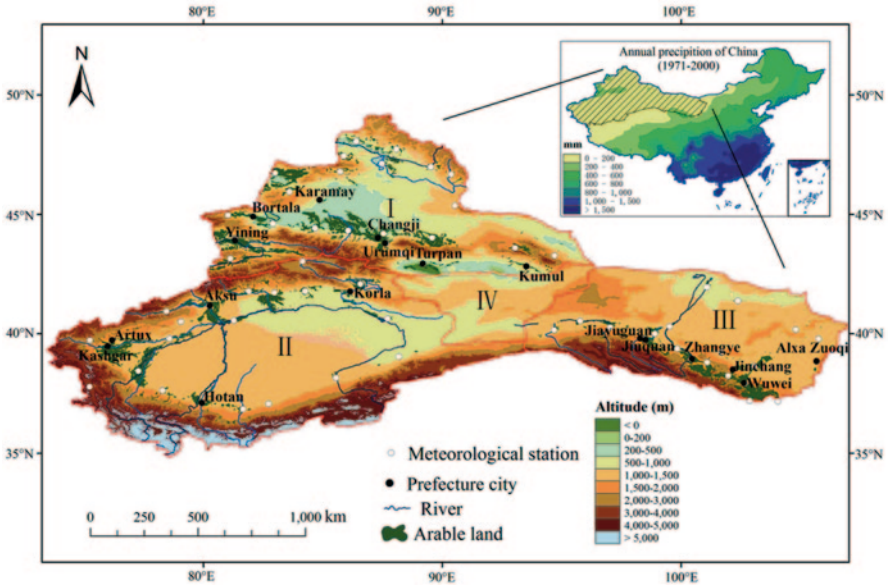


Fig. 1.1 The geomorphologic setting and zoning of the arid region in Northwestern China

Region (Xinjiang for short), the Hexi Corridor in Gansu Province, and the western portion of the Helan Mountains in Inner Mongolia. The land mass comprises approximately 2.5 million km<sup>2</sup> and accounts for one quarter of the total land area of China (Fig. 1.1). It is a major component of the arid region of Central Asia and also the typical region of desert in the world.

The Northwest arid area is bounded to the south by the Kunlun Mountains and Qilian Mountains, north by the Altai Mountains (Fig. 1.1). These ranges, together with the Tibetan Plateau, effectively block the Indian Ocean moisture from reaching the Northwest. Likewise, the Altai Mountain to the north prevents moisture from the Arctic Ocean from reaching the area.

Xinjiang is divided by the Tianshan Mountains into two parts: north and south. Conventionally, the area south of the Tianshan Mountains is called South Xinjiang and the area to the north is called North Xinjiang. To the east, the Helan Mountains block the moisture from the eastern monsoons. The area north of Qilian Mountain and west of the Helan Mountains are known as the Hexi Corridor.

Northwest China arid zone has diverse and extreme terrain. Its typical topography and geomorphology patterns include towering glaciers, widespread deserts (e.g., the Gobi), vast grasslands, sporadic oases, and numerous mountains and basins. The Tarim River Basin, which is China's largest, spans an area of approximately 530,000 m<sup>2</sup>. Additionally, China's largest (and the world's second-largest) mobile desert, the Taklimakan Desert, is in the central portion of the basin. The Turpan Basin, in eastern Xinjiang, has an elevation of -145 m, making it the lowest natural point in the country. The Tarim River and the Heihe River are, respectively, China's longest and second longest inland rivers.

As well as being diverse and made up of extremes, the Northwest arid area is a secluded inland region featuring a continental climate. Being very dry, the region tends to evaporate all precipitation it does receive, the average annual precipitation being only 130 mm (Chen et al. 2009). Because precipitation in the plains area does not produce surface runoff, this is one of the most severely arid areas in the world. The ecological environment is fragile and unstable, and species are extremely poor. Moreover, as the area is situated far from the sea, moisture is unable to reach it (Li 2012). Instead, precipitation mainly occurs in the Yili River Valley (an area strongly influenced by westerlies), north of the Altai Mountains (which is influenced by Arctic Ocean water vapor), or at the edge of the Hexi Corridor region. The highest precipitation levels (up to 800 mm) occur in the eastern mountains of the Yili Valley (Park et al. 2010; Wu et al. 2010; Ye et al. 2000; Yuan et al. 2003; Zhong et al. 2007, 2010).

In light of the area's large geographical span and unique landscape pattern, precipitation and water resources are unevenly distributed (Chen et al. 2009). Some oases with agricultural production activities have annual precipitation of less than 50 mm, with potential evaporation of up to 2,500 or 3,000 mm, which is 50–60 times the average precipitation. Clearly, the arid region of Northwest China can easily be described as one of the world's most arid regions.

The snow and glaciers coating the Northwest mountains give birth to more than 600 rivers. Other than for the Irtysh River in northern Xinjiang (which is part of the Arctic Ocean water system), all are inland rivers. Due to scant river runoff and closed terrain conditions, no tributaries pour into the main stream and the waters flow mainly through deserts until finally evaporating. The major rivers in this area are the Tarim River, the Yili River, the Irtysh River, the Heihe River, and the Shiyang River.

The Yili River originates in the Tianshan Mountains and is fed by high levels of precipitation due to the effect of the prevailing westerlies. The annual runoff of the Yili is 17 billion m<sup>3</sup>, making it the largest in the region (Ye et al. 1996). The Tarim River Basin is composed of the Aksu River, the Hotan River, the Yarkand River and the Kaidu-Kongque River. Measuring 2,179 km in length, the Tarim River is China's longest inland river, and flows from west to east through the northern basin. All of these rivers, along with numerous streams, are products of glacier snowmelt water. They wind through the arid region's oases and serve as the main source of irrigation water for local farmland.

The Northwest features a large diurnal temperature range with adequate heat and light sources, making it suitable for thermophilic plants and crops. However, because of the large geographic span from north to south and the uneven spatial distribution of heat resources, there are significant differences in the cropping systems and crop varieties. In southern Xinjiang, and where heat resources permit, cotton is grown and there are both summer and winter wheat crops. In contrast, the cooler climes of northern Xinjiang and the Hexi Corridor yield only one annual growing season, the main crops being wheat and spring corn. The uneven spatial distribution of heat resources directly impacts inter-regional differences in crop growth periods.

Currently, Northwest China is the main gathering point for ethnic minorities. Despite harboring a vast and rich supply of minerals, oil, gas and other natural resources, the area remains underdeveloped but is slated to become an important

resource replacement for China in the twenty-first century. Indeed, with the focus of national economic construction moving ever westward, the arid zone has become the fulcrum for China's economic growth. However, the resources presently in place to support the development of the ecological environment are inadequate, and the conflict of water utilization is very conspicuous. How to achieve sustainable use of resources in the Northwest, along with ecologically sustainable management and sustainable economic and social development, has become the focus of attention of all levels of government as well as the affected communities.

### **1.1.1 Landform Features**

As outlined above, the arid area of Northwest China is a vast territory of complex topography that includes mountains, plateaus, deserts and basins, with mountain runoff supplying most of the water resources. From a macroeconomic viewpoint, the region is mainly composed of large basins (the Tarim, Junggar and Turpan-Hami Basins and the Hexi Corridor) and continuous mountain ranges (the Tianshan, Karakoram, Kunlun, Qilian and Altai Mountains).

#### **1.1.1.1 Terrain**

Generally speaking, the terrain in the Northwest arid zone is high in the west and low in the east. In the mountainous western area, which features the Qilian, Kunlun, Tianshan and Altai Mountains, some peaks reach as high as 7,000 m. The foot of the Qilian Mountain is connected to the Alashan Plateau and the Hexi Corridor, the latter which forms part of the depression zone at the edge of the Qilian Mountains and is about 1,000 km long. The piedmont sloping plains, composed of numerous alluvial fans of the Qilian Mountains. These plains, situated among the Heli Hill and the Longshou and Qilian Mountains, are between 1,000 and 1,500 m above sea level.

Being located west of the Yellow River, the Hexi Corridor terrain tilts from southeast to northwest and is an important road leading to the Western Regions from eastern China. Historically, the famous ancient "Silk Road" passed through there and it is still the main road connecting eastern China with Xinjiang. Although the annual precipitation is less than 200 mm, the abundant snowmelt from the Qilian Mountains enables irrigation, thereby creating the mainstay agricultural base of the Northwest territories (Zhao et al. 1995).

The Alashan region is high and flat. It belongs to the temperate dry desert region, which is 1,000–1,500 m above sea level. In winter, this area is strongly influenced by high pressure centered on Mongolia, and so the climate is more arid than in the Junggar Basin. However, in summer, the southeast is impacted by Pacific monsoons, bringing sudden and thunderous showers. Annual precipitation in the region hovers around 200 mm, while the lower reaches of the Heihe River receive only about 50 mm. The main desert vegetation is made up of extremely sparse shrubs and semi-shrub desert (Zhao et al. 1995).